ELSEVIER

Journal of Fluids and Structures 26 (2010) 377–392

JOURNAL OF FLUIDS AND STRUCTURES

www.elsevier.com/locate/jfs

Free vibration analysis of a finite circular cylindrical shell in contact with unbounded external fluid

Moon K. Kwak*

Department of Mechanical, Robotics and Energy Engineering, Dongguk University-Seoul, 26 Pil-Dong 3-Ga, Joong-Gu, Seoul 100-715, Republic of Korea

Received 5 June 2009; accepted 19 January 2010
Available online 26 February 2010

Abstract

The free flexural vibration of a finite cylindrical shell in contact with external fluid is investigated. The fluid is assumed to be inviscid and irrotational. The cylindrical shell is modeled by using the Rayleigh–Ritz method based on the Donnell–Mushtari shell theory. The fluid is modeled based on the baffled shell model, which is applied to fluid–structure interaction problems. The kinetic energy of the fluid is derived by solving the boundary-value problem. The natural vibration characteristics of the submerged cylindrical shell are discussed with respect to the added virtual mass approach. In this study, the nondimensionalized added virtual mass incremental factor for the submerged finite shell is derived. This factor can be readily used to estimate the change in the natural frequency of the shell due to the presence of the external fluid. Numerical results showed the efficacy of the proposed method, and comparison with previous results showed the validity of the theoretical results.

Keywords: Cylindrical shell; Hydroelasticity; Added virtual mass

1. Introduction

Cylindrical shells filled with fluid are the practical elements of many types of engineering structures such as airplanes, ships and construction buildings. External fluid plays an important role in various industrial fields such as submarine construction, aeronautics or vibration control of nuclear reactors. Therefore, it becomes very important to analyze the vibration characteristics of shells in contact with fluid.

The equations of motion for the cylindrical shell *in vacuo* have been derived by means of many theories, each based on different assumptions (e.g. Markus (1988)). The simplest theory on the behavior of the thin cylindrical shell is the Donnell–Mushtari theory (e.g. Leissa (1993)). In light of increasing interest in active vibration suppression of cylindrical shell structures (Clark and Fuller, 1991), a dynamic model of the cylindrical shell structure suitable for vibration suppression control was derived by Kwak et al. (2009) based on the Donnell–Mushtari theory. The equations of motion were expressed in matrix form suitable for control design.

The natural vibration characteristics of the fluid-filled shells have been extensively studied (Amabili et al., 1998, 1999, 2003; Amabili and Touze, 2007; Karagiozis et al., 2005; Zhang et al., 2001a, b). On the other hand, the theoretical study

*Tel.: +82 2 2260 3705; fax: +82 2 2263 9379.
E-mail address: kwakm@dongguk.edu

0889-9746/$ - see front matter © 2010 Elsevier Ltd. All rights reserved.
doi:10.1016/j.jfluidstructs.2010.01.006

of a finite cylindrical shells coupled with unbounded external fluid has focused on acoustic radiation from a vibrating shell. Although many solution methods for fluid–structure interaction problems of the cylindrical shell in contact with either an internal fluid or an external fluid have been proposed, it is very difficult to mathematically analyze the effect of an external fluid on the natural vibration characteristics of the cylindrical shell structure. As demonstrated in (Kwak, 1991, 1997), analytical approaches have been limited to a few types of problems such as hydroelastic vibration of circular plates.

A simple approach to solving fluid–structure interaction problems of a cylindrical shell in contact with external fluid is to consider the cylindrical shell as being infinite so that the problem can be reduced to two-dimensions. Bleich and Baron (1954) adopted this approach and studied the vibrations of an infinitely long cylindrical shell in contact with an external fluid. Endo and Tosaka (1989) studied the free vibrations of an infinitely long cylindrical shell under axisymmetric hydrodynamic pressures arising from external and internal fluids. Amabili (1997) applied the added virtual mass approach to study infinitely long cylindrical shells partially coupled with external and internal fluids.

The analytical approach, however, cannot be applied to the coupled problem of a finite cylindrical shell submerged in a fluid because of the boundary conditions at both ends. A popular approximate approach for studying the vibro-acoustical behavior of a submerged finite cylindrical shell considers a baffled shell (Sandman, 1976; Stepanishen, 1982; Laulagnet and Cyuader, 1989; Harari and Sandman, 1990; Mattei, 1995; Berot and Peseux, 1998), which implies that semi-infinite rigid cylinders are attached to both ends of the finite cylindrical elastic shell. Although this model is not realistic, it does allow us to derive an analytical expression for the fluid effect on the vibro-acoustical behavior of the finite cylindrical shell. Zhang et al. (2001a, b) investigated the effects of the baffles and end-caps on the coupled structural–acoustical behaviors of finite cylindrical shells by using the finite element and the boundary element method. They considered the finite shell to be enclosed by either two plate end-caps or two semi-sphere end-caps, and they compared the results with those for the baffled shell model. Their results showed that the coupled natural frequencies are nearly the same for the three models and the sound radiation is only affected by the baffles over a small distance close to the shell ends. Hence, it can be said that it is possible to use a finite baffled cylindrical shell to model a submerged finite cylindrical shell. Zhang (2002) employed the wave propagation approach to analyze the natural frequencies of submerged cylindrical shells and presented a method for the estimation of the coupled frequency. Amabili et al. (1999) also discussed the effect of boundary conditions at the shell extremities on the nonlinear dynamics and stability of circular cylindrical shells containing fluid flow. However, the equations of motion in matrix form suitable for vibration control design of a submerged finite circular cylindrical shell have not yet been presented.

Many researchers who study the vibro-acoustical behavior of the baffled cylindrical shell have focused only on the derivation of the impedance or far-field pressure of the fluid caused by the vibrations of the shell; therefore, the resulting equations of motion are not suitable for use in designing the vibration suppression control of submerged cylindrical shells. Furthermore, it has been difficult to estimate the change of the natural frequency of the cylindrical shell due to the presence of the external fluid. One can resort to the finite element method or the boundary element method to analyze fluid–structure interaction problems. However, these numerical approaches give us only quantitative results. In this study, the added virtual mass matrix for the submerged cylindrical shell is derived by using the Rayleigh–Ritz approach based on the baffled shell assumption. With this matrix, we can easily compute the natural vibration characteristics of the finite cylindrical shell in contact with a fluid and derive equations of motion suitable for the design of vibration suppression controls.

2. Kinetic and potential energies for a cylindrical shell *in vacuo*

The dynamic model of the circular cylindrical shell, as shown in Fig. 1, was derived in (Kwak et al., 2009). In Fig. 1, R is the radius of the cylindrical shell mid-surface, h is the thickness, L is the length, θ is the angle with respect to the vertical axis, x is the axis along the length of the cylinder, and u, v and w are the mid-surface displacements in the x, θ and z directions, respectively. The kinetic energy for the cylindrical shell is expressed as (Leissa, 1993)

$$T_s = \frac{1}{2}\rho \int_0^L \int_0^{2\pi} \int_{-h/2}^{h/2} (\dot{u}^2 + \dot{v}^2 + \dot{w}^2) R\, dz\, d\theta\, dx, \tag{1}$$

where ρ is the mass density of the cylindrical shell. It is assumed that u, v and w are not functions of z, the material properties of the shell are homogeneous and isotropic, and z is the distance to an arbitrary point on the shell from the middle surface. According to Donnell's shell theory, equations for strain and stress are needed to obtain the potential

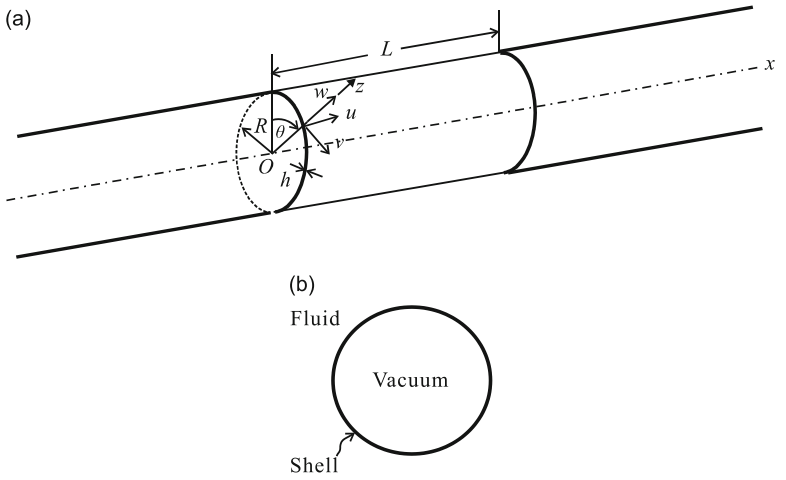

Fig. 1. Coordinate system for the baffled cylindrical shell. (a) Coordinates of baffled cylindrical shell and (b) unbounded external fluid domain.

energy of the cylindrical shell, which are expressed as (Blevins, 1987)

$$\varepsilon_x = \frac{\partial u}{\partial x} - z\frac{\partial^2 w}{\partial x^2}, \quad \varepsilon_\theta = \frac{1}{R}\frac{\partial v}{\partial \theta} + \frac{w}{R} - \frac{z}{R^2}\frac{\partial^2 w}{\partial \theta^2}, \quad \varepsilon_{x\theta} = \frac{\partial v}{\partial x} + \frac{1}{R}\frac{\partial u}{\partial \theta} - \frac{2z}{R}\frac{\partial^2 w}{\partial x\,\partial \theta}, \tag{2a, b, c}$$

$$\varepsilon_{xz} = \varepsilon_{\theta z} = \varepsilon_{zz} = 0, \tag{2d}$$

$$\sigma_x = \frac{E}{1-\nu^2}(\varepsilon_x + \nu\varepsilon_\theta), \quad \sigma_\theta = \frac{E}{1-\nu^2}(\varepsilon_\theta + \nu\varepsilon_x), \quad \sigma_{x\theta} = \sigma_{\theta x} = \frac{E}{2(1+\nu)}\varepsilon_{x\theta}, \tag{3a, b, c}$$

$$\sigma_{xz} = \sigma_{\theta z} = \sigma_{zz} = 0, \tag{3d}$$

where E is the Young's modulus and ν is Poisson's ratio. The out-of-plane shear strains are assumed to be zero. The stresses in the shell follow isotropic stress–strain relationships. The elastic strain energy of a circular cylindrical shell, neglecting stress, σ_{zz} according to Love's first approximations, and out-of-plane shear stress is given by (Leissa, 1993)

$$V_s = \frac{1}{2}\int_0^L \int_0^{2\pi} \int_{-h/2}^{h/2} (\sigma_x\varepsilon_x + \sigma_\theta\varepsilon_\theta + \sigma_{x\theta}\varepsilon_{x\theta}) R\,dz\,d\theta\,dx. \tag{4}$$

Inserting Eqs. (2) and (3) into Eq. (4) results in the following equation for the potential energy (Leissa, 1993):

$$\begin{aligned} V_s = \frac{ERh}{2(1-\nu^2)}\int_0^L \int_0^{2\pi} \Bigg[& \left(\frac{\partial u}{\partial x}\right)^2 + \frac{h^2}{12}\left(\frac{\partial^2 w}{\partial x^2}\right)^2 + \frac{1}{R^2}\left(\frac{\partial v}{\partial \theta}\right)^2 + \frac{w^2}{R^2} + \frac{h^2}{12R^4}\left(\frac{\partial^2 w}{\partial \theta^2}\right)^2 + \frac{2}{R^2}\left(\frac{\partial v}{\partial \theta}\right)w + \frac{2\nu}{R}\left(\frac{\partial u}{\partial x}\right)\left(\frac{\partial v}{\partial \theta}\right) \\ & + \frac{2\nu}{R}\left(\frac{\partial u}{\partial x}\right)w + \frac{\nu h^2}{6R^2}\left(\frac{\partial^2 w}{\partial x^2}\right)\left(\frac{\partial^2 w}{\partial \theta^2}\right) + \frac{(1-\nu)}{2}\left(\frac{\partial v}{\partial x}\right)^2 + \frac{(1-\nu)}{2R^2}\left(\frac{\partial u}{\partial \theta}\right)^2 + \frac{(1-\nu)h^2}{6R^2}\left(\frac{\partial^2 w}{\partial x\partial \theta}\right)^2 \\ & + \frac{(1-\nu)}{R}\left(\frac{\partial v}{\partial x}\right)\left(\frac{\partial u}{\partial \theta}\right)\Bigg] d\theta\,dx. \end{aligned} \tag{5}$$

For vibration analysis, let us express the displacement in each direction as the series of functions which have n circumferential nodes:

$$u(x,\theta,t) = \sum_{n=0}^{\infty} u_n(x,\theta,t), \quad v(x,\theta,t) = \sum_{n=0}^{\infty} v_n(x,\theta,t), \quad w(x,\theta,t) = \sum_{n=0}^{\infty} w_n(x,\theta,t). \tag{6a–c}$$

when $n = 0$, the cylindrical shell vibrates without nodal points, and its natural frequencies are higher than those of the cylindrical shell with circumferential nodal points. Hence, we consider the case when $n \geq 1$ in the numerical calculation.

The mathematical derivation for the free vibration analysis is exactly the same as in (Kwak et al., 2009) except for the circumferential mode. Only the following expansions for each function in Eq. (6) are coupled (Kwak et al., 2009). Hence, for free vibration analysis we can write

$$u_n(x,\theta,t)=\mathbf{\Phi}_u(x)\cos n\theta\mathbf{q}_{nu}(t),\ \ v_n(x,\theta,t)=\mathbf{\Phi}_v(x)\sin n\theta\mathbf{q}_{nv}(t),\ \ w_n(x,\theta,t)=\mathbf{\Phi}_w(x)\cos n\theta\mathbf{q}_{nw}(t), \tag{7a–c}$$

where

$$\mathbf{\Phi}_u(x)=[\Phi_{u1}(x)\,\Phi_{u2}(x)\ldots\Phi_{um}(x)],\ \ \mathbf{\Phi}_v(x)=[\Phi_{v1}(x)\,\Phi_{v2}(x)\ldots\Phi_{vm}(x)],\ \ \mathbf{\Phi}_w(x)=[\Phi_{w1}(x)\Phi_{w2}(x)\ldots\Phi_{wm}(x)], \tag{7d–f}$$

$$\mathbf{q}_{nu}(t)=[q_{nu1}(t)\,q_{nu1}(t)\ldots q_{num}(t)]^{\mathrm{T}},\ \ \mathbf{q}_{nv}(t)=[q_{nv1}(t)q_{nv1}(t)\ldots q_{nvm}(t)]^{\mathrm{T}},\ \ \mathbf{q}_{nw}(t)=[q_{nw1}(t)\,q_{nw1}(t)\ldots q_{nwm}(t)]^{\mathrm{T}}, \tag{7g–i}$$

in which $\mathbf{\Phi}_u(x)$, $\mathbf{\Phi}_v(x)$, $\mathbf{\Phi}_w(x)$ represent a matrix consisting of admissible functions in each direction, $\mathbf{q}_{nu}(t)$, $\mathbf{q}_{nv}(t)$, $\mathbf{q}_{nw}(t)$ are generalized coordinate vectors corresponding to the cosine and sine modes, and m is the number of admissible functions used for the longitudinal expansion. It should be noted that other sets of cosine and sine modes should be considered for response calculations and control designs (Kwak et al., 2009).

Before inserting Eq. (6) into Eqs. (1) and (5), let us introduce the following nondimensional variables to facilitate the numerical analysis:

$$\xi=x/L,\quad \alpha=L/R,\quad \beta=h/R. \tag{8a–c}$$

Because the displacements are expressed in series expansions of functions corresponding to each circumferential mode, the kinetic and potential energies of the shell *in vacuo* can be expressed as

$$T=\sum_{n=1}^{\infty}T_{sn},\quad V=\sum_{n=1}^{\infty}V_{sn}, \tag{9a, b}$$

where T_{sn} and V_{sn} are the kinetic and potential energies corresponding to the nth circumferential mode, respectively. Considering Eqs. (7) and (8), and inserting Eq. (6) into Eqs. (1) and (5), the kinetic and potential energies corresponding to the $n(\geq 1)$th circumferential mode can be derived as follows (Kwak et al., 2009):

$$T_{sn}=\frac{1}{2}\rho RhL\pi(\dot{\mathbf{q}}_{nu}^{\mathrm{T}}\mathbf{M}_{uu}\dot{\mathbf{q}}_{nu}+\dot{\mathbf{q}}_{nv}^{\mathrm{T}}\mathbf{M}_{vv}\dot{\mathbf{q}}_{nv}+\dot{\mathbf{q}}_{nw}^{\mathrm{T}}\mathbf{M}_{ww}\dot{\mathbf{q}}_{nw}), \tag{10}$$

$$V_{sn}=\frac{\pi ERh}{(1-\nu^2)L}\left(\frac{1}{2}\mathbf{q}_{nu}^{\mathrm{T}}\mathbf{K}_{nuu}\mathbf{q}_{nu}+\frac{1}{2}\mathbf{q}_{nv}^{\mathrm{T}}\mathbf{K}_{nvv}\mathbf{q}_{nv}+\frac{1}{2}\mathbf{q}_{nw}^{\mathrm{T}}\mathbf{K}_{nww}\mathbf{q}_{nw}+\mathbf{q}_{nu}^{\mathrm{T}}\mathbf{K}_{nuv}\mathbf{q}_{nv}+\mathbf{q}_{nv}^{\mathrm{T}}\mathbf{K}_{nvw}\mathbf{q}_{nw}+\mathbf{q}_{nu}^{\mathrm{T}}\mathbf{K}_{nuw}\mathbf{q}_{nw}\right), \tag{11}$$

where

$$\mathbf{M}_{uu}=\mathbf{\Phi}_{uu},\quad \mathbf{M}_{vv}=\mathbf{\Phi}_{vv},\quad \mathbf{M}_{ww}=\mathbf{\Phi}_{ww}, \tag{12a–c}$$

$$\mathbf{K}_{nuu}=\overline{\mathbf{\Phi}}_{uu}+\frac{(1-\nu)\alpha^2n^2}{2}\mathbf{\Phi}_{uu},\quad \mathbf{K}_{nvv}=\alpha^2n^2\mathbf{\Phi}_{vv}+\frac{(1-\nu)}{2}\overline{\mathbf{\Phi}}_{vv}, \tag{12d, e}$$

$$\mathbf{K}_{nww}=\alpha^2\mathbf{\Phi}_{ww}+\frac{\beta^2}{12}\left(\frac{\hat{\mathbf{\Phi}}_{ww}}{\alpha^2}+\alpha^2n^4\mathbf{\Phi}_{ww}-2\nu n^2\tilde{\mathbf{\Phi}}_{ww}+2(1-\nu)n^2\overline{\mathbf{\Phi}}_{ww}\right), \tag{12f}$$

$$\mathbf{K}_{nuv}=\nu n\alpha\tilde{\mathbf{\Phi}}_{uv}-\frac{(1-\nu)\alpha n}{2}\hat{\mathbf{\Phi}}_{uv},\quad \mathbf{K}_{nuw}=\nu\alpha\tilde{\mathbf{\Phi}}_{uw},\quad \mathbf{K}_{nvw}=\alpha^2n\mathbf{\Phi}_{vw}, \tag{12g–i}$$

in which

$$\mathbf{\Phi}_{uu}=\int_0^1 \mathbf{\Phi}_u^{\mathrm{T}}\mathbf{\Phi}_u\,\mathrm{d}\xi,\quad \mathbf{\Phi}_{vv}=\int_0^1 \mathbf{\Phi}_v^{\mathrm{T}}\mathbf{\Phi}_v\,\mathrm{d}\xi,\quad \mathbf{\Phi}_{ww}=\int_0^1 \mathbf{\Phi}_w^{\mathrm{T}}\mathbf{\Phi}_w\,\mathrm{d}\xi,\quad \mathbf{\Phi}_{vw}=\int_0^1 \mathbf{\Phi}_v^{\mathrm{T}}\mathbf{\Phi}_w\,\mathrm{d}\xi, \tag{13a–d}$$

$$\overline{\mathbf{\Phi}}_{uu}=\int_0^1 \mathbf{\Phi}'^{\mathrm{T}}_u\mathbf{\Phi}'_u\,\mathrm{d}\xi,\quad \overline{\mathbf{\Phi}}_{vv}=\int_0^1 \mathbf{\Phi}'^{\mathrm{T}}_v\mathbf{\Phi}'_v\,\mathrm{d}\xi,\quad \overline{\mathbf{\Phi}}_{ww}=\int_0^1 \mathbf{\Phi}'^{\mathrm{T}}_w\mathbf{\Phi}'_w\,\mathrm{d}\xi,\quad \tilde{\mathbf{\Phi}}_{uv}=\int_0^1 \mathbf{\Phi}'^{\mathrm{T}}_u\mathbf{\Phi}_v\,\mathrm{d}\xi, \tag{13e–h}$$

$$\tilde{\mathbf{\Phi}}_{uw}=\int_0^1 \mathbf{\Phi}'^{\mathrm{T}}_u\mathbf{\Phi}_w\,\mathrm{d}\xi,\quad \tilde{\mathbf{\Phi}}_{ww}=\int_0^1 \mathbf{\Phi}''^{\mathrm{T}}_w\mathbf{\Phi}_w\,\mathrm{d}\xi,\quad \hat{\mathbf{\Phi}}_{uv}=\int_0^1 \mathbf{\Phi}^{\mathrm{T}}_u\mathbf{\Phi}'_v\,\mathrm{d}\xi,\quad \hat{\mathbf{\Phi}}_{ww}=\int_0^1 \mathbf{\Phi}''^{\mathrm{T}}_w\mathbf{\Phi}''_w\,\mathrm{d}\xi. \tag{13i–l}$$

3. Fluid–structure interaction

Let us consider the cylindrical shell located in a baffle of a rigid cylinder, as shown in Fig. 1. The governing equation for the fluid in contact with the shell is the Laplace equation which is given by

$$\nabla^2\phi=0. \tag{14}$$

The fluid is assumed to be inviscid, incompressible and irrotational. In the case of the baffled shell, the boundary condition at the fluid–structure interface is as follows:

$$\frac{\partial\phi}{\partial r}=\begin{cases}-\dot{w}(x,\theta,t) & \text{at } r=R,\ 0\le x\le L,\\ 0 & \text{at } r=R,\ \text{otherwise.}\end{cases} \tag{15}$$

Eq. (15) shows why infinitely long rigid cylinders are connected to both ends of the cylindrical shell. Otherwise, the addressed problem cannot be solved by the analytical approach. The velocity potential must also satisfy the radiation conditions which imply that the velocity potential should converge to zero

$$\phi,\frac{\partial\phi}{\partial r},\frac{\partial\phi}{\partial x}\to 0 \text{ as } x,r\to\infty. \tag{16}$$

If we express the velocity potential in terms of the series expansion of the velocity potential for each circumferential mode as we do for the shell deflection in Eq. (6), we can write

$$\phi(r,x,\theta,t)=\sum_{n=1}^{\infty}\phi_n(r,x,\theta,t), \tag{17}$$

where

$$\phi_n(r,x,\theta,t)=\cos n\theta\ \mathbf{\Psi}_n(r,x)\dot{\mathbf{q}}_{nw}(t), \tag{18}$$

in which $\mathbf{\Psi}_n(r,x)=\begin{bmatrix}\Psi_{n1} & \Psi_{n2} & \dots & \Psi_{nm}\end{bmatrix}$ represents the vector of the admissible potential function corresponding to each generalized coordinate. Each velocity potential should also satisfy the Laplace equation so that we can obtain the following equation by inserting Eq. (18) into Eq. (14):

$$\frac{\partial^2\Psi_{ni}}{\partial r^2}+\frac{1}{r}\frac{\partial\Psi_{ni}}{\partial r}-\frac{n^2}{r^2}\Psi_{ni}+\frac{\partial^2\Psi_{ni}}{\partial x^2}=0,\quad i=1,2,\dots,m. \tag{19}$$

Let us introduce the Fourier transform of each potential function defined as

$$\overline{\Psi}_{ni}(r,\xi)=\int_{-\infty}^{\infty}\Psi_{ni}(r,x)\mathrm{e}^{-\mathrm{j}\xi x}\,dx. \tag{20}$$

Applying the Fourier transform, Eq. (20), into Eq. (19) results in

$$\frac{d^2\overline{\Psi}_{ni}}{dr^2}+\frac{1}{r}\frac{d\overline{\Psi}_{ni}}{dr}-\left(\frac{n^2}{r^2}+\xi^2\right)\overline{\Psi}_{ni}=0. \tag{21}$$

The general solution of Eq. (21) is found to be

$$\overline{\Psi}_{ni}(r,\xi) = A_{ni}\mathrm{I}_n(|\xi|r) + B_{ni}\mathrm{K}_n(|\xi|r), \tag{22}$$

where I_n, K_n are modified Bessel functions of the first and second kind, respectively. The radiation condition, Eq. (16), implies that the potential should decay exponentially. Hence, we can write

$$\overline{\Psi}_{ni}(r,\xi) = B_{ni}\mathrm{K}_n(|\xi|r). \tag{23}$$

Inserting Eq. (17) into Eq. (15) and using Eqs. (7c) and (18) results in

$$\frac{\partial\Psi_{ni}}{\partial r} = \begin{cases} -\Phi_{wi} & \text{at } r = R,\ 0 \le x \le L, \\ 0 & \text{at } r = R, \text{ otherwise.} \end{cases} \tag{24}$$

Applying the Fourier transform to Eq. (24) leads to

$$\left.\frac{d\overline{\Psi}_{ni}(r,\xi)}{dr}\right|_{r=R} = -\int_0^L \Phi_{wi}(x)\mathrm{e}^{-\mathrm{j}\xi x}\,dx. \tag{25}$$

Hence, the unknown coefficient of the general solution can be obtained by inserting Eq. (23) into Eq. (25):

$$B_n = \frac{-1}{d\mathrm{K}_n(|\xi|r)/dr|_{r=R}}\int_0^L \Phi_{wi}(x)\mathrm{e}^{-\mathrm{j}\xi x}\,dx. \tag{26}$$

By inserting Eq. (26) into Eq. (23), we can then obtain the Fourier transform of the velocity potential function in closed form

$$\overline{\Psi}_{ni}(r,\xi) = \frac{-\mathrm{K}_n(|\xi|r)}{d\mathrm{K}_n(|\xi|r)/dr|_{r=R}}\int_0^L \Phi_{wi}(x)\mathrm{e}^{-\mathrm{j}\xi x}\,dx. \tag{27}$$

The inverse Fourier transform is expressed as

$$\Psi_{ni}(r,\xi) = \frac{1}{2\pi}\int_{-\infty}^{\infty} \overline{\Psi}_{ni}(r,x)\mathrm{e}^{\mathrm{j}\xi x}\,d\xi. \tag{28}$$

Inserting Eq. (27) into Eq. (28) results in

$$\Psi_{ni}(r,x) = \frac{-1}{2\pi}\int_{-\infty}^{\infty} \frac{\mathrm{K}_n(|\xi|r)}{d\mathrm{K}_n(|\xi|r)/dr|_{r=R}}\int_0^L \Phi_{wi}(\overline{x})\mathrm{e}^{-\mathrm{j}\xi\overline{x}}\,d\overline{x}\mathrm{e}^{\mathrm{j}\xi x}\,d\xi. \tag{29}$$

Using the symmetry condition, we can express the above equation as follows:

$$\Psi_{ni}(r,x) = \frac{-1}{\pi}\int_0^{\infty} \frac{\mathrm{K}_n(\xi r)}{d\mathrm{K}_n(\xi r)/dr|_{r=R}}\int_0^L \Phi_{wi}(\overline{x})\cos\xi(x-\overline{x})\,d\overline{x}\,d\xi. \tag{30}$$

Eqs. (30) and (18) can be used to compute the velocity potential at an arbitrary location in three-dimensional fluid space. Let us derive the kinetic energy of the fluid due to the vibration of the shell. The kinetic energy of a fluid is expressed as follows:

$$T_f = -\frac{1}{2}\rho_f\int_0^{2\pi}\int_0^L \left(\phi\frac{\partial\phi}{\partial r}\right)_{r=R} dx\,R\,d\theta, \tag{31}$$

where ρ_f is the mass density of the fluid. Using Eqs. (15), (17) and (30), Eq. (31) turns out to be

$$T_f = \sum_{n=1}^{\infty} T_{fn} = \sum_{n=1}^{\infty} \frac{1}{2} \dot{\mathbf{q}}_{nw}^{\mathrm{T}} \mathbf{M}_{fwn} \dot{\mathbf{q}}_{nw}, \tag{32}$$

where

$$\mathbf{M}_{fwn} = \rho_f R\pi \int_0^L \mathbf{\Psi}_{fn}^{\mathrm{T}} \mathbf{\Phi}_w|_{r=R}\, dx \tag{33}$$

represents the added virtual mass matrix due to the presence of the fluid and the element of the matrix can be expressed as

$$(\mathbf{M}_{fwn})_{ij} = \rho_f R \int_0^{\infty} \frac{-\mathrm{K}_n(\xi R)}{d\mathrm{K}_n(\xi r)/dr|_{r=R}} \int_0^L \int_0^L \Phi_{wi}(\overline{x})\Phi_{wj}(x)\cos\xi(x-\overline{x})\, d\overline{x}\, dx\, d\xi. \tag{34}$$

Introducing nondimensional variables, $x = L\eta$, $\overline{x} = L\overline{\eta}$, $\overline{\xi} = R\xi$, in addition to Eq. (8), into Eqs. (33) and (34), we can obtain

$$\mathbf{M}_{fwn} = \rho_f RL^2 \pi \overline{\mathbf{M}}_{fwn}, \tag{35}$$

where the element of the nondimensionalized mass matrix can be expressed as

$$(\overline{\mathbf{M}}_{fwn})_{ij} = \frac{1}{\pi} \int_0^{\infty} \frac{-\mathrm{K}_n(\overline{\xi})}{\left(-\overline{\xi}\mathrm{K}_{n+1}(\overline{\xi}) + n\mathrm{K}_n(\overline{\xi})\right)} \int_0^1 \int_0^1 \Phi_{wi}(\eta)\Phi_{wj}(\overline{\eta})\cos\overline{\xi}(x-\overline{\eta})\, d\overline{\eta}\, d\eta\, d\overline{\xi}. \tag{36}$$

We have derived the analytical expression for the added virtual mass matrix as shown above. However, the above expression consists of triple integrals and does not permit a closed-form solution, so a numerical integration technique needs to be used to compute the added virtual mass matrix. The integral limits of $\overline{\xi}$ become a concern when doing the numerical integration. Numerical computations demonstrated that the integrand of Eq. (36) quickly converges to zero as $\overline{\xi}$ becomes large. It was also found from the asymptotic property of the Bessel function that the integrand has the following limit as $\overline{\xi}$ goes to zero:

$$\frac{-\mathrm{K}_n(\overline{\xi})}{\left(-\overline{\xi}\mathrm{K}_{n+1}(\overline{\xi}) + n\mathrm{K}_n(\overline{\xi})\right)} \to \frac{1}{n} \quad \text{as} \quad \overline{\xi} \to 0. \tag{37}$$

These two properties of the integrand were used when evaluating the integral, Eq. (36), numerically.

The total kinetic energy for the nth circumferential mode is the summation of the kinetic energy of the shell and the kinetic energy of the fluid

$$T_n = T_{sn} + T_{fn}. \tag{38}$$

Inserting Eqs. (10) and (32) into Eq. (38) and using Eq. (35), we can obtain

$$T_n = \frac{1}{2}\rho RhL\pi[\dot{\mathbf{q}}_{nu}^{\mathrm{T}}\mathbf{M}_{uu}\dot{\mathbf{q}}_{nu} + \dot{\mathbf{q}}_{nv}^{\mathrm{T}}\mathbf{M}_{vv}\dot{\mathbf{q}}_{nv} + \dot{\mathbf{q}}_{nw}^{\mathrm{T}}(\mathbf{M}_{ww} + \gamma\overline{\mathbf{M}}_{fwn})\dot{\mathbf{q}}_{nw}], \tag{39}$$

where $\gamma = \rho_f L/\rho h$ is the nondimensional factor. Eq. (39) shows that the added virtual mass due to the presence of the fluid appears in the z-directional motion.

4. Eigenvalue problem

Considering the kinetic and potential energy expressions given by Eqs. (11) and (39), the free vibrations of the cylindrical shell in fluid for the nth circumferential mode can be derived as follows:

$$(\rho RhL\pi)(\mathbf{M}_a + \gamma\mathbf{M}_{fn})\ddot{\mathbf{q}}_n + \frac{ERh\pi}{(1-\nu^2)L}\mathbf{K}_n\mathbf{q}_n = 0, \quad n = 1, 2, \ldots, \tag{40}$$

where $\mathbf{q}_n(t) = [\mathbf{q}_{nu}^{\mathrm{T}}\ \mathbf{q}_{nv}^{\mathrm{T}}\ \mathbf{q}_{nw}^{\mathrm{T}}]^{\mathrm{T}}$ and

$$\mathbf{M}_a = \begin{bmatrix} \mathbf{M}_{uu} & 0 & 0 \\ 0 & \mathbf{M}_{vv} & 0 \\ 0 & 0 & \mathbf{M}_{ww} \end{bmatrix},\ \mathbf{M}_{fn} = \begin{bmatrix} 0 & 0 & 0 \\ 0 & 0 & 0 \\ 0 & 0 & \overline{\mathbf{M}}_{fwn} \end{bmatrix},\ \mathbf{K}_n = \begin{bmatrix} \mathbf{K}_{nuu} & \mathbf{K}_{nuv} & \mathbf{K}_{nuw} \\ \mathbf{K}_{nuv}^{\mathrm{T}} & \mathbf{K}_{nvv} & \mathbf{K}_{nvw} \\ \mathbf{K}_{nuw}^{\mathrm{T}} & \mathbf{K}_{nvw}^{T} & \mathbf{K}_{nww} \end{bmatrix}. \tag{41a–c}$$

The eigenvalue problem for each circumferential mode can then be written as follows:

$$[\mathbf{K}_n - \overline{\omega}_{fn}^2(\mathbf{M}_a + \gamma\mathbf{M}_{fn})]\mathbf{q}_n = 0, \quad n = 1, 2, \ldots, \tag{42}$$

where $\overline{\omega}_{fn} = \omega_{fn}\sqrt{\rho(1-\nu^2)L^2/E}$ represents the nondimensionalized natural frequency in fluid.

Let us consider the eigenvalue problem of the cylindrical shell vibrating *in vacuo*. In this case, we have

$$[\mathbf{K}_n - \overline{\omega}_{an}^2\mathbf{M}_a]\mathbf{q}_n^a = 0, \quad n = 1, 2, \ldots \tag{43}$$

The eigenvalue problem admits the following orthonormality conditions:

$$\mathbf{U}_n^{\mathrm{T}}\mathbf{K}_n\mathbf{U}_n = \overline{\mathbf{\Omega}}_{an}^2, \quad \mathbf{U}_n^{\mathrm{T}}\mathbf{M}_a\mathbf{U}_n = \mathbf{I}. \tag{44}$$

If we apply the modal transformation, $\mathbf{q}_n = \mathbf{U}_n\boldsymbol{\varsigma}_n$, to the eigenvalue problem of the cylindrical shell vibrating in the fluid, Eq. (42), and pre-multiply it by $\mathbf{U}_n^{\mathrm{T}}$, we can obtain

$$[\overline{\mathbf{\Omega}}_{an}^2 - \overline{\mathbf{\Omega}}_{fn}^2(\mathbf{I} + \gamma\overline{\mathbf{M}}_{fn})]\boldsymbol{\varsigma}_n = 0, \quad n = 1, 2, \ldots, \tag{45}$$

where $\overline{\mathbf{M}}_{fn} = \mathbf{U}_n^{\mathrm{T}}\mathbf{M}_{fn}\mathbf{U}_n$. If we assume that the natural mode of the cylindrical shell does not change in the fluid, which implies that $\overline{\mathbf{M}}_{fn}$ is a diagonally dominant matrix, we may simplify Eq. (45):

$$(\omega_{fn})_i = \frac{(\omega_{an})_i}{\sqrt{1+\gamma\Gamma_{ni}}}, \quad i, n = 1, 2, \ldots, \tag{46}$$

where $\Gamma_{ni} = (\overline{\mathbf{M}}_{fn})_{ii}$ represents the so-called nondimensionalized added virtual mass incremental (NAVMI) factor. This formula can be effectively used to estimate the change of the natural frequency due to the presence of the fluid.

5. Numerical results

As a numerical example, a cylindrical shell under the shear diaphragm boundary condition at both ends is considered. In this case, the boundary conditions at both ends are

$$v = w = M_x = N_x = 0. \tag{47}$$

The admissible functions that satisfy the above boundary conditions can be expressed as (Leissa, 1993)

$$\Phi_{ui}(x) = \sqrt{2}\cos\frac{i\pi x}{L}, \quad \Phi_{vi}(x) = \Phi_{wi}(x) = \sqrt{2}\sin\frac{i\pi x}{L}, \quad i = 1, 2, \ldots, m \tag{48}$$

Inserting Eq. (48) into Eq. (13) and inserting the results into Eq. (12), we can calculate the mass and stiffness matrices for each nth circumferential mode. Furthermore, inserting Eq. (48) into Eq. (36), we can calculate the added virtual mass matrix due to the fluid effect. It was found from numerical experiments that the infinite integral limit of Eq. (36) can be replaced by 10 with sufficient accuracy.

Figs. 2–6 show the nondimensionalized natural frequencies of the cylindrical shell *in vacuo* for each circumferential mode when $\beta = 0.01$. Figs. 7–11 show the nondimensionalized natural frequencies of the cylindrical shell *in vacuo* for each circumferential mode when $\beta = 0.02$. As shown in Figs. 2–11, the radius-to-length ratio, α, greatly affect the natural frequencies but the effect of the thickness-to-radius ratio, β, on the natural frequencies is not significant for small values of β.

Figs. 12–16 show the nondimensionalized added virtual mass incremental (NAVMI) factor that appeared in Eq. (46) for each circumferential mode when $\beta = 0.01$. The NAVMI factor did not change significantly when β was changed to 0.02, so the case of $\beta = 0.02$ was omitted. As shown in Figs. 12–16, the NAVMI factors decrease monotonically as α

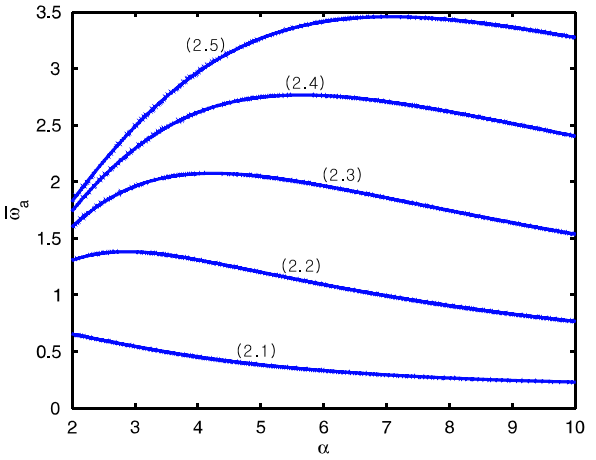

Fig. 2. Nondimensionalized natural frequency ($n = 2$, $\beta = 0.01$).

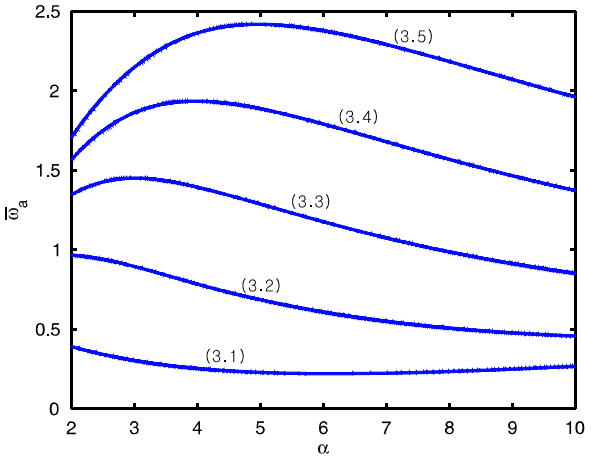

Fig. 3. Nondimensionalized natural frequency ($n = 3$, $\beta = 0.01$).

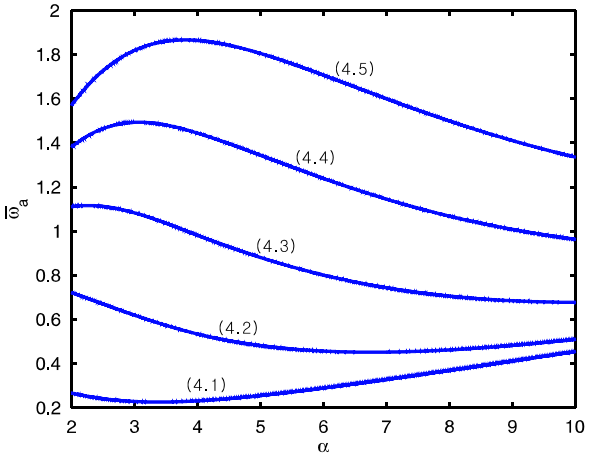

Fig. 4. Nondimensionalized natural frequency ($n = 4$, $\beta = 0.01$).

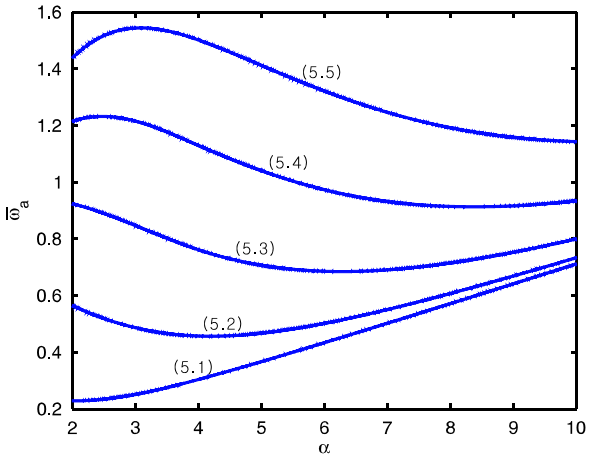

Fig. 5. Nondimensionalized natural frequency ($n = 5$, $\beta = 0.01$).

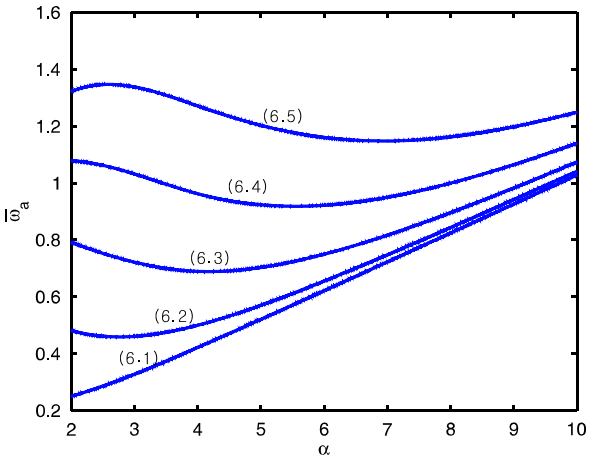

Fig. 6. Nondimensionalized natural frequency ($n = 6$, $\beta = 0.01$).

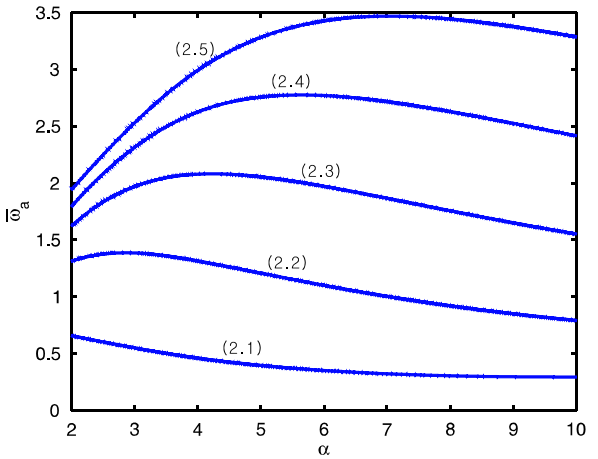

Fig. 7. Nondimensionalized natural frequency ($n = 2$, $\beta = 0.02$).

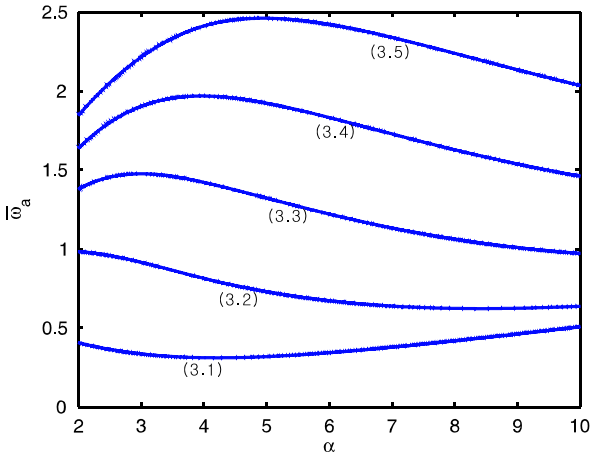

Fig. 8. Nondimensionalized natural frequency ($n = 3$, $\beta = 0.02$).

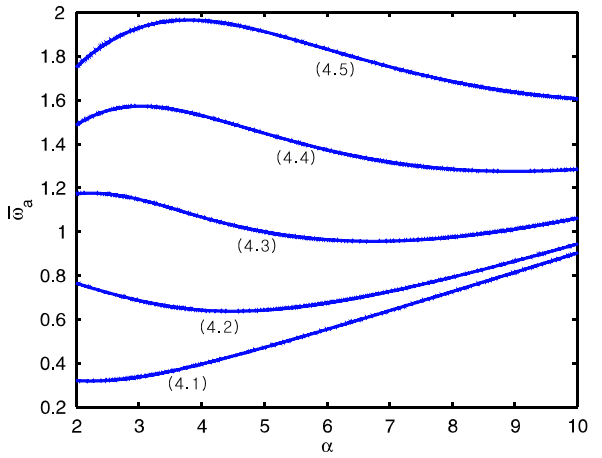

Fig. 9. Nondimensionalized natural frequency ($n = 4$, $\beta = 0.02$).

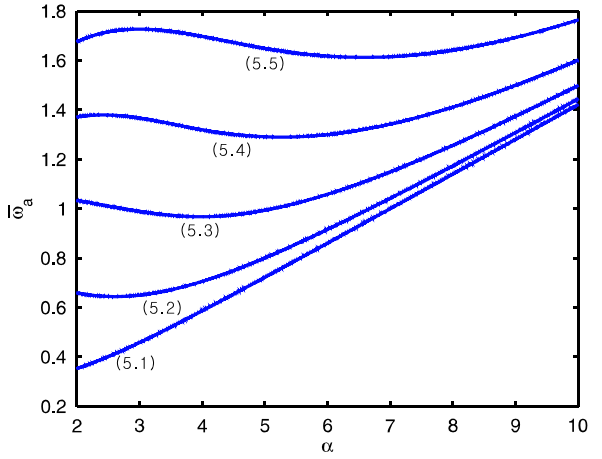

Fig. 10. Nondimensionalized natural frequency ($n = 5$, $\beta = 0.02$).

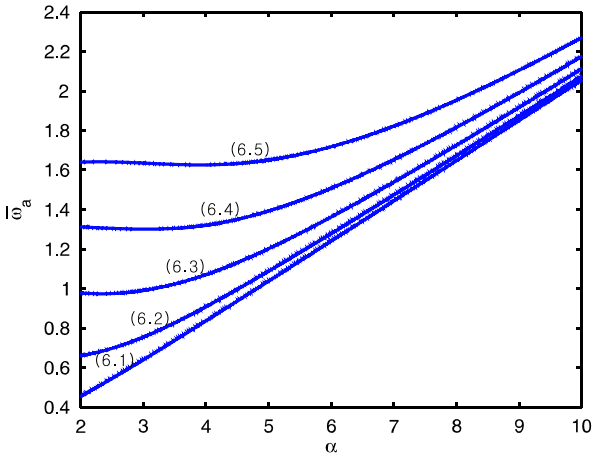

Fig. 11. Nondimensionalized natural frequency ($n = 6$, $\beta = 0.02$).

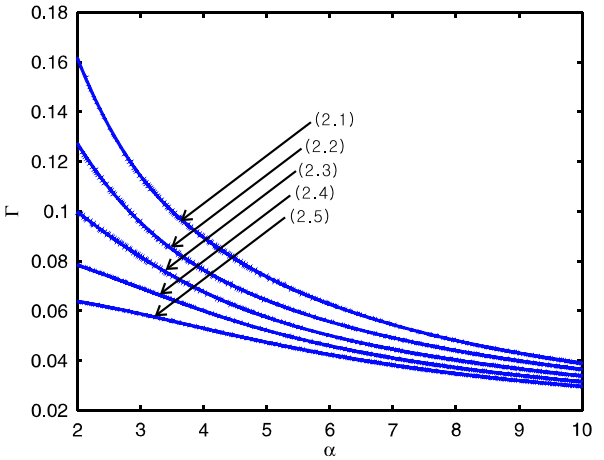

Fig. 12. Nondimensionalized added virtual incremental factor ($n = 2$, $\beta = 0.01$).

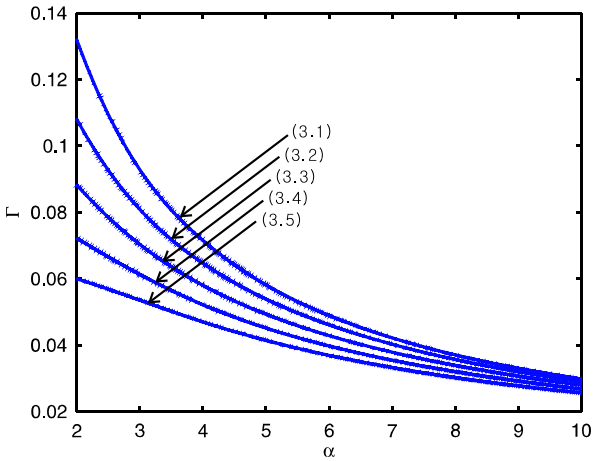

Fig. 13. Nondimensionalized added virtual incremental factor ($n = 3$, $\beta = 0.01$).

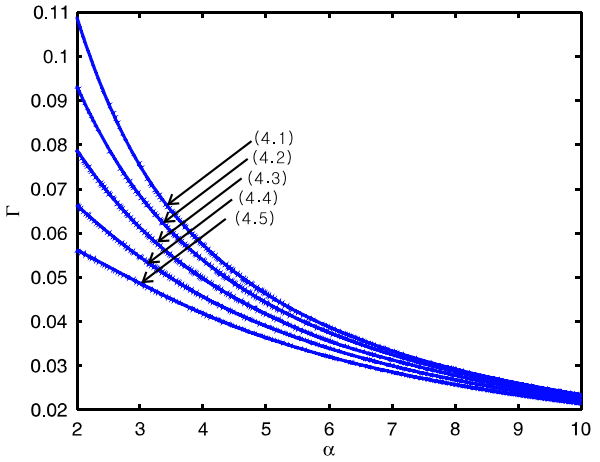

Fig. 14. Nondimensionalized added virtual incremental factor ($n = 4$, $\beta = 0.01$).

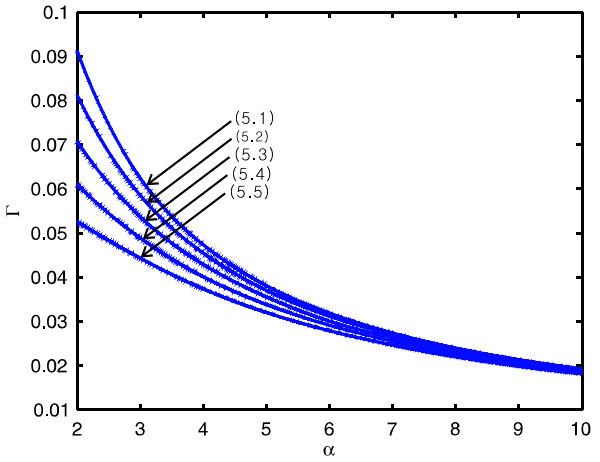

Fig. 15. Nondimensionalized added virtual incremental factor ($n = 5$, $\beta = 0.01$).

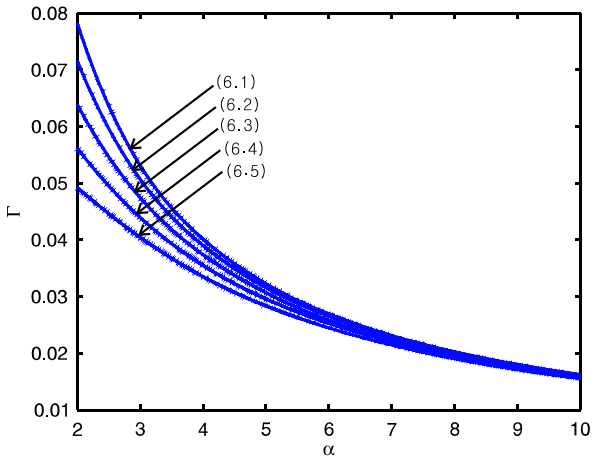

Fig. 16. Nondimensionalized added virtual incremental factor ($n = 6$, $\beta = 0.01$).

Table 1
Comparison of natural frequencies *in vacuo*.

Mode	Berot and Peseux (1998)	Current method
(5,1)	142.9 Hz	142.86
(4,1)	145.7	145.73
(6,1)	176.7	176.67
(3,1)	210.4	210.36
(7,1)	230.1	230.13
(6,2)	281.1	281.14
(7,2)	290.8	290.79
(8,1)	296.3	296.28

Table 2
Comparison of natural frequencies in water.

Mode	Berot and Peseux (1998)	Current method
(4,1)	66.4 Hz	66.25
(5,1)	69.9	69.84
(3,1)	88.5	87.84
(6,1)	91.8	91.76
(7,1)	125.8	125.76
(6,2)	148.8	148.50
(2,1)	149.7	146.37
(7,2)	161.1	160.85

increases. This implies that the effect of the fluid on the natural frequencies decreases as the length of the shell increases. The NAVMI factors decrease as the number of circumferential modes increases. In addition, the NAVMI factors in each circumferential mode decrease as the order of natural frequency increases, which implies that the effect of the fluid is significant for lower natural frequencies, as concluded in other cases (Amabili, 1997; Kwak, 1997).

The nondimensionalized natural frequencies of the cylindrical shell *in vacuo* shown in Figs. 2–11, along with the NAVMI factors shown in Figs. 12–16, can be effectively used in the estimation of the natural frequencies of the submerged cylindrical shell. For instance, once the dimension and material properties of the cylindrical shell are known, the natural frequencies *in vacuo* can be easily read from Figs. 2–11 and the NAVMI factors can be read from Figs. 12–16. The natural frequencies of the immersed cylindrical shell can then be determined by using the simple formula, Eq. (46). If the natural frequencies of the cylindrical shell *in vacuo* are measured by vibration testing, then the natural frequencies of the cylindrical shell in fluid can be estimated by using the simple formula, Eq. (46).

For comparison, natural frequencies obtained by the current method are compared to those obtained by Berot and Peseux (1998). The shell considered by Berot and Peseux (1998) has the following material properties: $L = 1.2\,\text{m}$, $h = 0.003\,\text{m}$, $R = 0.4\,\text{m}$, $E = 200\,\text{GPa}$, $v = 0.3$, $\rho = 7850\,\text{kg/m}^3$, $\rho_f = 1000\,\text{kg/m}^3$. Table 1 shows the natural frequencies *in vacuo* and Table 2 shows the natural frequencies in water. Natural frequencies in air obtained by the current method are the same as those obtained by Berot and Peseux (1998). This is obvious because Berot and Peseux (1998) also used the Donnell–Mushtari theory. As shown in Table 2, the natural frequencies obtained by the current method are almost equal to those obtained by Berot and Peseux (1998), except for the sequence of the (2,1) and (6,2) modes. However, the natural frequencies of the (2,1) and (6,2) modes are close to each other, so that their sequence is not a substantial problem in real applications.

6. Summary and conclusions

In this study, the hydroelastic behavior of the cylindrical shell was discussed. The equations of motion for the cylindrical shell were derived using the Rayleigh–Ritz method and presented in matrix form, which were suitable for

predicting changes in the natural frequencies and for the design of vibration suppression controls. The effect of the fluid on the equations of motion appears as the added virtual mass matrix. In this study, the added mass matrix reflecting the presence of the fluid was derived by assuming a baffled shell and solving the Laplace equation by applying the Fourier transform method. Based on the assumption that the natural modes of the cylindrical shell do not change due to the presence of the fluid, the nondimensionalized added virtual mass incremental (NAVMI) factor was derived.

Numerical computations were carried out for the cylindrical shell with a shear diaphragm at both ends. The effect of the fluid on the natural frequencies of the cylindrical shell decreased as the length of the shell increased, and the fluid affected the lower natural frequencies to a great extent. Nondimensionalized natural frequencies and the NAVMI factors were presented as graphs, which can be effectively used in the estimation of the natural frequencies of cylindrical shells in a fluid.

Comparison with previous work shows the efficacy of the proposed method.

Acknowledgements

This study was supported by a research grant from the Underwater Vehicle Research Center of Defense Acquisition Program Administration and Agency for Defense Development, Korea. This financial support is gratefully acknowledged.

References

Amabili, M., 1997. Flexural vibration of cylindrical shells partially coupled with external and internal fluids. ASME Journal of Vibration and Acoustics 119, 476–484.

Amabili, M., Pellicano, F., Paidoussis, M.P., 1998. Nonlinear vibrations of simply supported, circular cylinderical shells, coupled to quiescent fluid. Journal of Fluids and Structures 12, 883–918.

Amabili, M., Pellicano, F., Paidoussis, M.P., 1999. Non-linear dynamics and stability of circular cylindrical shells containing flowing fluid. Part I: Stability. Journal of Sound and Vibration 225 (4), 655–699.

Amabili, M., Sarkar, A., Paidoussis, M.P., 2003. Reduced-order models for nonlinear vibrations of cylindrical shells via the proper orthogonal decomposition method. Journal of Fluids and Structures 18, 227–250.

Amabili, M., Touze, C., 2007. Reduced-order models for nonlinear vibrations of fluid-filled circular cylindrical shells: comparison of POD and asymptotic nonlinear normal modes methods. Journal of Fluids and Structures 23, 885–903.

Berot, F., Peseux, B., 1998. Vibro-acoustic behaviour of submerged cylindrical shells: analytical formulation and numerical model. Journal of Fluids and Structures 12, 959–1003.

Bleich, H.H., Baron, M.L., 1954. Vibrations of an infinitely long cylindrical shell in an infinite acoustic medium. Journal of Applied Mechanics 76, 167.

Blevins, R.D., 1987. Formulas for Natural Frequency and Mode Shape. Robert E. Krieger Publishing Co., Inc., FL.

Clark, R.L., Fuller, C.R., 1991. Active control of structurally radiated sound from an enclosed finite cylinder. In: Proceedings of the Conference on Recent Advances in Active Control of Sound and Vibration. Virginia Polytechnic Institute and State University, Blacksburg, VA, pp. 380–402.

Endo, R., Tosaka, N., 1989. Free vibration analysis of coupled external fluid-elastic cylindrical shell-internal fluid systems. JSME International Journal, Series I 2, 217–221.

Harari, A., Sandman, B.E., 1990. Radiation and vibrational properties of submerged stiffened cylindrical shells. Journal of Acoustical Society of America 88 (4), 1817–1830.

Karagiozis, K.N., Amabili, M., Paidoussis, M.P., Misra, A.K., 2005. Nonlinear vibrations of fluid-filled clamped circular cylindrical shells. Journal of Fluids and Structures 21, 579–595.

Kwak, M.K., 1991. Vibration of circular plates in contact with water. Journal of Applied Mechanics 58 (2), 480–483.

Kwak, M.K., 1997. Hydroelastic vibration of circular plates. Journal of Sound and Vibration 201, 293–303.

Kwak, M.K., Heo, S., Jeong, M., 2009. Dynamic modelling and active vibration controller design for a cylindrical shell equipped with piezoelectric sensors and actuators. Journal of Sound and Vibration 321, 510–524.

Laulagnet, B., Cyuader, J.L., 1989. Modal analysis of a shell's acoustic radiation in light and heavy fluids. Journal of Sound and Vibration 131 (3), 397–415.

Leissa, A., 1993. Vibration of Shells. Acoustical Society of America, Originally issued by NASA 1973.

Markus, S., 1988. The Mechanics of Vibrations of Cylindrical Shells, Studies in Applied Mechanics, vol. 17. Elsevier.

Mattei, P.-O., 1995. Sound radiation by a baffled shell: comparison of the exact and an approximate solution. Journal of Sound and Vibration 188 (1), 111–130.

Sandman, B.E., 1976. Numerical fluid loading coefficients for the modal velocities of a cylindrical shell. Computers and Structures 6, 467–473.

Stepanishen, P.R., 1982. Modal coupling in the vibration of fluid-loaded cylindrical shells. Journal of Acoustical Society of America 71 (4), 813–823.

Zhang, X.M., 2002. Frequency analysis of submerged cylindrical shells with the wave propagation approach. International Journal of Mechanical Sciences 44, 1259–1273.

Zhang, X.M., Liu, G.R., Lam, K.Y., 2001a. The effects of baffles and end-caps on coupled vibration and sound radiation of finite cylindrical shells. International Journal of Engineering Simulation 2, 19–25.

Zhang, X.M., Liu, G.R., Lam, K.Y., 2001b. Coupled vibration analysis of fluid-filled cylindrical shells using the waver propagation approach. Applied Acoustics 62, 229–243.